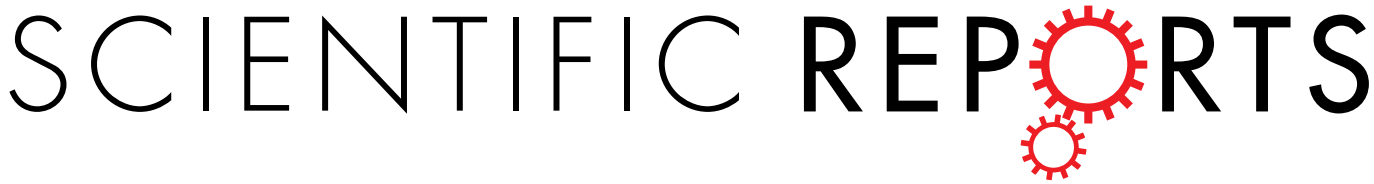

OPEN

# Saturation-Recovery Myocardial $T_1$-Mapping during Systole: Accurate and Robust Quantification in the Presence of Arrhythmia

Received: 27 February 2017
Accepted: 5 March 2018
Published online: 27 March 2018

Nadja M. Meßner[1,2], Johannes Budjan[3], Dirk Loßnitzer[4], Theano Papavassiliu[2,4], Lothar R. Schad[1], Sebastian Weingärtner[1,5,6] & Frank G. Zöllner[1]

**Myocardial $T_1$-mapping, a cardiac magnetic resonance imaging technique, facilitates a quantitative measure of fibrosis which is linked to numerous cardiovascular symptoms. To overcome the problems of common techniques, including lack of accuracy and robustness against partial-voluming and heart-rate variability, we introduce a systolic saturation-recovery $T_1$-mapping method. The Saturation-Pulse Prepared Heart-rate independent Inversion-Recovery (SAPPHIRE) $T_1$-mapping method was modified to enable imaging during systole. Phantom measurements were used to evaluate the insensitivity of systolic $T_1$-mapping towards heart-rate variability. *In-vivo* feasibility and accuracy were demonstrated in ten healthy volunteers with native and post-contrast $T_1$-mappping during systole and diastole. To show benefits in the presence of RR-variability, six arrhythmic patients underwent native $T_1$-mapping. Resulting systolic SAPPHIRE $T_1$-values showed no dependence on arrhythmia in phantom (CoV $<$ 1%). *In-vivo*, significantly lower $T_1$ (1563 $\pm$ 56 ms, precision: 84.8 ms) and ECV-values (0.20 $\pm$ 0.03) than during diastole ($T_1$ = 1580 $\pm$ 62 ms, p = 0.0124; precision: 60.2 ms, p = 0.03; ECV = 0.21 $\pm$ 0.03, p = 0.0098) were measured, with a strong correlation of systolic and diastolic $T_1$ (r = 0.89). In patients, mis-triggering-induced motion caused significant imaging artifacts in diastolic $T_1$-maps, whereas systolic $T_1$-maps displayed resilience to arrythmia. In conclusion, the proposed method enables saturation-recovery $T_1$-mapping during systole, providing increased robustness against partial-voluming compared to diastolic imaging, for the benefit of $T_1$-measurements in arrhythmic patients.**

Cardiac magnetic resonance imaging enables the assessment of cardiac anatomy and function and the detection of myocardial fibrosis, which is linked to numerous cardiovascular adverse cardiovascular events like heart failure, arrhythmia and sudden cardiac death[1]. In addition to late gadolinium enhancement as a robust standard for focal fibrosis, even diffuse cardiac pathologies can now be assessed with $T_1$-mapping, the non-invasive alternative to biopsy[2].

$T_1$-maps are obtained by acquiring multiple sample points on a longitudinal magnetization recovery curve after magnetization preparation. Imaging at the same cardiac phase yields co-registered images, henceforth referred to as base-images, and pixel-wise curve fitting allows for spatially resolved quantification of $T_1$[3]. Pre- and post-contrast $T_1$-mapping further permit estimation of the extracellular volume (ECV) fraction. Both biomarkers have shown to be predictors of mortality in cardiovascular disease and bear promise for risk stratification[4].

However, partial-volume effects at the interface between myocardium and blood-pool corrupt quantification accuracy and impair reproducibility in $T_1$-mapping[5,6]. Hence, imaging during systole, exploiting increased

[1]Computer Assisted Clinical Medicine, Medical Faculty Mannheim, Heidelberg University, Mannheim, Germany. [2]DZHK (German Centre for Cardiovascular Research) partner site Heidelberg/Mannheim, Mannheim, Germany. [3]Department of Clinical Radiology and Nuclear Medicine, University Medical Center Mannheim, Medical Faculty Mannheim, Heidelberg University, Mannheim, Germany. [4]1st Department of Medicine Cardiology, University Medical Center Mannheim, Medical Faculty Mannheim, Heidelberg University, Mannheim, Germany. [5]Department of Electrical and Computer Engineering, University of Minnesota, Minneapolis, MN, United States. [6]Center for Magnetic Resonance Research, University of Minnesota, Minneapolis, MN, United States. Sebastian Weingärtner and Frank G. Zöllner jointly supervised this work. Correspondence and requests for materials should be addressed to S.W. (email: sebastian.weingaertner@medma.uni-heidelberg.de)

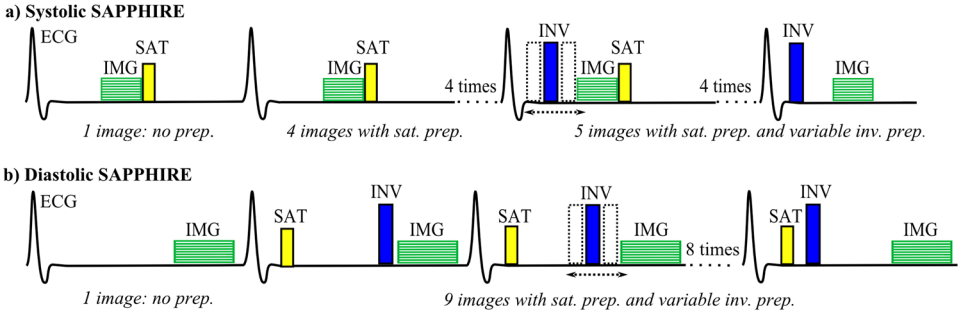


**Figure 1.** Sequence diagrams of the systolic (**a**) and diastolic (**b**) SAPPHIRE $T_1$-mapping sequence with ten readouts, as used in phantom and in healthy volunteers. Systolic $T_1$-mapping starts with one image (IMG) without preparation, the following four images (seven images in patients) are preceded by a saturation pulse (SAT) in the heart beat before imaging, directly after the previous image acquisition. The remaining images (four in healthy, seven in patients) are acquired with an additional inversion-pulse (INV) with variable delay after the R-wave. (**b**) In diastolic (conventional) SAPPHIRE, the first image acquisition is also performed without magnetization preparation. However, for the remaining images, both the saturation- and the inversion-pulse are played within the same heartbeat before image acquisition. The image acquisition window is longer compared with systole.

myocardial thickness, has recently been proposed[7] and demonstrated improved quality in patients with atrial fibrillation[8]. However, the modified Look-Locker inversion recovery (IR) technique (MOLLI)[3] was used in these studies, which is known to underestimate $T_1$-values[9], and to be affected by the patient's heart-rate[10] and various imaging parameters[11]. Alternatively, saturation-recovery (SR) $T_1$-mapping, as realized by the Saturation-recovery single-shot acquisition (SASHA)[12] technique, provides more accurate $T_1$-values, for the trade-off against reduced precision. A hybrid version of IR and SR, called Saturation-Pulse Prepared Heart-rate independent Inversion-Recovery (SAPPHIRE)[10], has been proposed to enable accurate $T_1$-quantification with increased precision compared to saturation-recovery only. However, systolic imaging cannot be performed with the previously proposed SASHA and SAPPHIRE sequences, as the preparation time between R-wave detection and systolic imaging is insufficient for magnetization recovery, leading to low SNR in base-images and compromising $T_1$-fit quality.

The purpose of this study is to develop a method for systolic saturation-recovery $T_1$-mapping and ECV-calculation at 3T and to provide robust image quality in patients suffering from arrhythmia.

## Materials and Methods

**Numerical Simulation.** The influence of mis-triggering artifacts on conventional SAPPHIRE $T_1$-maps was simulated in a $650 \times 650$ pixel numerical phantom, representing a mid-ventricular short-axis of the left-ventricular (LV) myocardium, left- and right-ventricular (RV) blood, and epicardial fat ($T_1 = 1578$; 2048; 382 ms, respectively)[13]. Systolic images were designed with reduced LV diameter (70%) and increased myocardial thickness (140%) (16). Ten base-images were generated by assigning signal values to the compartments calculated from Bloch simulations of the SAPPHIRE signal equation (inversion-times TI = [10000;805;113;211;309;407;505;603;701;799 ms]; trigger delay TD = 805 ms). Additive Gaussian noise was subsequently added (SNR = 60). Mis-triggering effects were mimicked by replacing diastolic by systolic base-images in randomized order. The share of systolic images was calculated in terms of four arrhythmia factors, with standard deviations of 0%, 30%, 60%, and 70% of the mean RR length (667 ms), based on previous literature[14]. Each variant was simulated 50 times and analyzed for mean $T_1$ (accuracy) and standard-deviation across repetitions (precision).

**Systolic SAPPHIRE Sequence Design.** The proposed $T_1$-mapping variant consists of a hybrid saturation/inversion-recovery magnetization preparation and 10 ECG-triggered readouts (in patients 15 readouts, respectively). The average scan time in healthy subjects was 10 sec, in patients 12 sec, trading-off the higher number of images against the faster heart rate. In systole, the limited time between the R-wave and imaging yields insufficient signal for conventional SR $T_1$-mapping. To overcome this, the saturation-pulse is played in the preceding heartbeat after imaging (Fig. 1). The first image is acquired without preparation, yielding full recovery. Four images are acquired with saturation-preparation (WET module[13]) only, to obtain maximal recovery. Five images are additionally prepared with an inversion-pulse (adiabatic full passage tan/tanh pulse[15]) between the R-wave and image acquisition, with linearly spread inversion-times.

**Data Acquisition.** Images were acquired at a 3T MRI scanner (Magnetom Skyra; Siemens Healthcare, Erlangen, Germany) with a 30-channel receiver coil array. For systolic acquisition, a single-shot balanced Steady-State Free Precession (bSSFP) readout was used with the following parameters ("systolic parameter set"): TR/TE/$\alpha = 2.6$ ms/1.0 ms/35°, in-plane resolution $= 1.2 \times 1.2$ mm$^2$, slice-thickness = 6 mm, field-of-view $= 350 \times 263$ mm$^2$, bandwidth = 1240 Hz/px, #k-space-lines = 57, linear profile-ordering, startup-pulses = 5 Kaiser-Bessel, GRAPPA-factor = 3. Diastolic $T_1$-maps were acquired with longer acquisition windows using the following parameters ("diastolic parameter set): TR/TE/$\alpha = 2.6$ ms/1.0 ms/35°, in-plane resolution $= 1.7 \times 1.7$ mm$^2$, slice-thickness = 8 mm, field-of-view $= 440 \times 375$ mm$^2$, bandwidth = 1085 Hz/px,

| Patient N° | indication | Variability in RR length in ms | | |
|---|---|---|---|---|
| | | $RR_{mean} \pm std$ | $RR_{min}$ | $RR_{max}$ |
| 1 | ischemic cardiomyopathy, moderate reduced LV-function and a high burden of premature ventricular contraction | 816 ± 134 | 613 | 1068 |
| 2 | dilated cardiomyopathy with mild LV-dysfunction | 989 ± 275 | 665 | 1595 |
| 3 | coronary fistula with normal LV-function, but premature ventricular contration and bigeminy | 781 ± 136 | 618 | 973 |
| 4 | multifocal premature ventricular contractions on the Holter ECG | 1226 ± 69 | 1075 | 1308 |
| 5 | multifocal premature ventricular contractions on the Holter ECG | 1514 ± 426 | 890 | 2375 |
| 6 | coronary artery disease, atrial fibrillation and moderate reduced LV-function | 745 ± 224 | 560 | 1333 |

**Table 1.** Characteristics of the six arrhythmic patients (4 m, 52 ± 19 y) including their indications for cardiac MRI and their variability in RR length.

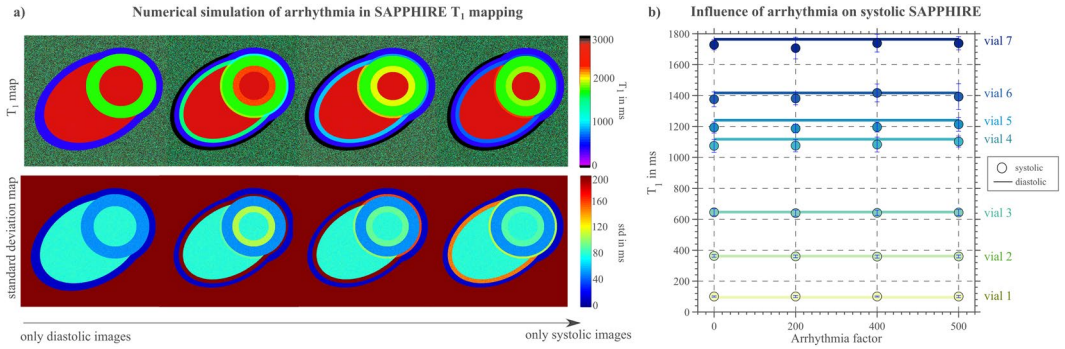


**Figure 2.** Influence of arrhythmia studied in (**a**) a numerical simulation and (**b**) in phantom measurements. (**a**) Simulated influence of arrhythmia on diastolic $T_1$-map quality is shown on a model mid-ventricular short-axis view and the corresponding standard deviation map. Blurring at the endo- and epicardial borders increased with increasing number of mis-triggered base-images. (**b**) Influence of simulated heart-rate variations on SAPPHIRE $T_1$-values for seven phantom vials covering a broad $T_1$-range. Circles indicate the $T_1$-results with systolic SAPPHIRE for four different arrhythmia factors (defined as the standard deviation from the Gaussian distribution of a mean RR-length of 1125 ms). Reference diastolic $T_1$-values are given as solid lines. No major influence of arrhythmia on systolic $T_1$-values was found.

#k-space-lines = 139, linear profile-ordering, startup-pulses = 5 Kaiser-Bessel, GRAPPA-factor = 2. Modified Look-Locker Inversion Recovery (MOLLI)[3] $T_1$-maps were acquired in the 5(3)3 scheme with the diastolic parameter set for both diastolic and systolic acquisition. For the latter, the acquisition window was shortened and shifted towards the systole.

**Phantom Experiments.** To study the influence of arrhythmia on $T_1$ in systole, scans were performed in seven vials containing agarose gel, doped with various concentrations of a gadoterate meglumine contrast agent (Dotarem; Guerbet, Aulnay-sous-Bois, France). Heart-rate variability was simulated by a pause of random duration before the R-wave, resulting in RR-interval standard-deviations of 0, 200, 400, and 500 ms, respectively.

***In Vivo* Experiments.** This prospective study was approved by the Institutional Review Board II, Medical Faculty Mannheim, Germany, and written informed consent was obtained from all volunteers. We hereby confirm that all experiments were performed in accordance with relevant guidelines and regulations.

As a preliminary substudy, five healthy volunteers (3 f, 26 ± 3 y) underwent native $T_1$-mapping with six different variants: (a) diastolic MOLLI, (b) systolic MOLLI, (c) diastolic SAPPHIRE with 'diastolic parameter set', (d) systolic SAPPHIRE with 'systolic parameter set', (e) systolic SAPPHIRE with 'diastolic parameter set' and shortened trigger delay and (f) systolic SAPPHIRE with 'systolic paramter set' and an increased number of base images (15 images).

Ten healthy volunteers (5 m, 25 ± 4 y) underwent $T_1$-mapping before and 15 min after injection of 0.2 mmol/kg Dotarem. $T_1$-maps were acquired in three short-axis slices during systole with the proposed method and during diastole with conventional SAPPHIRE. Timing for systolic acquisition was visually determined from short-axis cine images. To avoid a systematic influence of contrast agent washout, sequence and slice orders were randomized. Blood samples were drawn to measure blood hematocrit for ECV calculations.

Six patients (4 m, 52 ± 19 y) underwent native $T_1$-mapping in a mid-ventricular short-axis slice with systolic and diastolic SAPPHIRE. They partially displayed substantial arrhythmia during the scan, as can be seen in Table 1 on patient characteristics.

**Data Analysis and Statistics.** MATLAB R2014a (Mathworks; Natick, MA, USA) was used for image evaluation and statistics. For $T_1$-estimation, a 3-parameter least-squares fit to the $T_1$-recovery curve was performed.

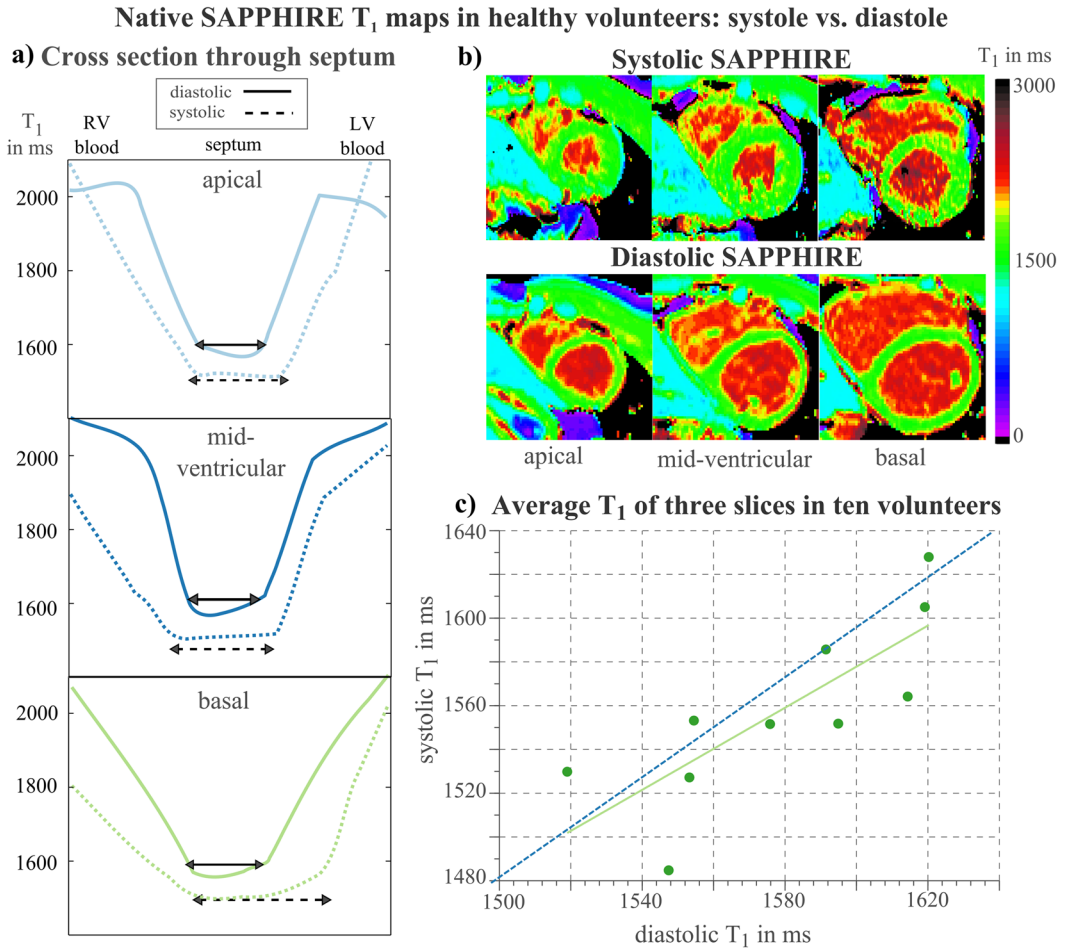


**Figure 3.** Reduction of partial-volume effects by higher myocardial thickness in systole. (**a**) Cross-sections through the LV septum in apical, mid-ventricular and basal short axis $T_1$-maps, acquired with systolic and diastolic SAPPHIRE. The cross-sections through diastolic $T_1$-maps (solid lines) show strongly elevated $T_1$-times at endo- and epicardial borders, whereas in systole (dotted), this effect is reduced. Corresponding $T_1$-maps of a healthy volunteer (m, 23 y) are shown in (**b**). The apparent myocardial thickness is clearly higher in systole compared to diastole, so more myocardial voxels can be included into $T_1$-estimation without risking an elevation of $T_1$-times by partial-volume effects from the highly intense blood-pool. (**c**) Correlation of systolic and diastolic native $T_1$ in ten healthy subjects, each point indicating the average over the three slices in each subject, revealing a strong positive correlation of the two methods. The identity line is indicated in dashed blue, the solid green line represents best fit.

$T_1$-map quality in numerical simulation was evaluated with standard-deviation maps. In phantom, $T_1$-times were analyzed in manually drawn ROIs. *In vivo*, pixel-wise fitting was performed to generate $T_1$-maps, followed by segmentation according to the AHA-16-segment-model[16], with estimation of $T_1$ and ECV as mean per segment. Precision was defined as the intra-segment variation in terms of standard-deviation. Blood $T_1$-times were evaluated from manually drawn ROIs in the LV-blood-pool. Diastolic $T_1$-maps were estimated with magnitude-images after polarity restoration[3]. Phase-sensitive fitting was used in systole by subtracting the phase of the non-magnetization-prepared base-image from the remaining images. The resulting phase difference was thresholded ($|\Delta\varphi| > \pi/2$ and $|\Delta\varphi| \leq \pi/2$) after phase unwrapping[17] to yield a signal polarity map, which was finally multiplied to all systolic base-images.

To assess the amount of myocardial tissue suited for $T_1$-evaluation, myocardial thickness was evaluated in healthy volunteers as the area between manually drawn LV endo- and epicardial borders in systole and diastole and in all slices. To estimate the effect of partial-voluming, the full-width-at-half-maximum (FWHM) of $T_1$-intensity line profiles from the LV to the RV blood-pool across the center of the septum was determined. The lack of a clearly depicted RV blood-pool in apical slices prevented their inclusion in the FWHM-analysis.

In phantom, a coefficient of variation (CoV) was calculated as the ratio of $T_1$-standard-deviation to mean $T_1$. For statistical comparison of systole and diastole *in vivo*, $T_1$- and ECV-values were studied with a paired student's t-test, and $T_1$-precision with a Mann–Whitney-U-test (significance for $p < 0.05$).

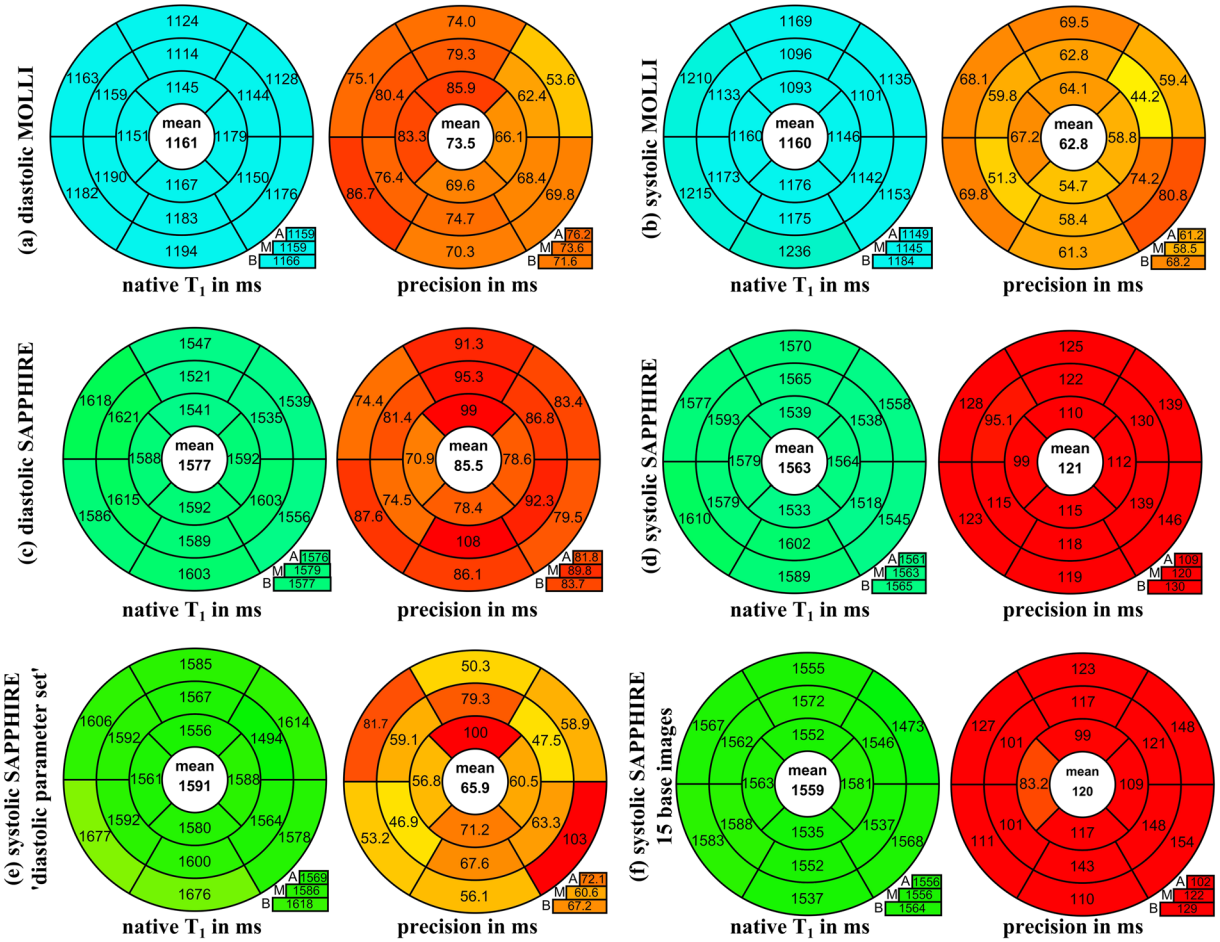


**Figure 4.** Indicative substudy for the comparison of MOLLI and SAPPHIRE sequence variants. Mean values of five healthy volunteers (3 f, 26 ± 3 y) in three short-axis slices (A = apical, M = mid-ventricular, B = basal) are displayed as bullseye plots (AHA-16-segment-model) for native myocardial $T_1$-times and $T_1$-time precision. They have been acquired with different sequence variants of the MOLLI and the SAPPHIRE $T_1$-mapping method. The average across all segments is given in the bullseye centers, slice averages in the boxes below.

## Results

Numerical simulations revealed a degrading effect of mis-triggering on conventional SAPPHIRE $T_1$-map quality in terms of blurring at myocardial borders, with increasing severity at higher degrees of arrhythmia (Fig. 2a). Accordingly, standard-deviation maps showed higher variation in border regions.

In phantom, systolic SAPPHIRE $T_1$-mapping results were independent of arrhythmia, as shown in Fig. 2b, yielding a CoV <1%.

*In vivo* $T_1$-mapping was successfully performed in all healthy subjects. bSSFP banding artifacts led to the exclusion of 26 out of 2080 segments (1.3%). Partial-volume effects showed a higher impact on diastolic than on systolic $T_1$-maps, as shown by a LV septal cross-section plot in Fig. 3a. In diastole, $T_1$-times at septal borders are clearly elevated towards the blood-pools, leaving only the inner region of the septum unaffected of partial-voluming. In systolic $T_1$-maps, however, larger plateaus for the estimation of myocardial $T_1$-times are available, as reflected by the significant increase in mean FWHM (mid-ventricular: 167 ± 37%; basal: 224 ± 89%) compared to diastole. Corresponding native $T_1$-maps of a healthy volunteer, where the increase in myocardial thickness from diastole to systole is clearly depicted, are shown in Fig. 3b. In average over all vounteers, the measured increase of myocardial thickness during systole is significant (apical: 255 ± 85%; mid-ventricular: 254 ± 63%; basal: 209 ± 40%; $p < 10^{-4}$). Systolic and diastolic $T_1$ display strong positive correlation (r = 0.89) (Fig. 3c).

The results of a preliminary comparison of different $T_1$-mapping results in five healthy volunteers are visualized in Fig. 4. Systolic MOLLI $T_1$-times ($T_1 = 1160 \pm 55$ ms, precision:62.8 ms) are significantly lower than systolic SAPPHIRE $T_1$-times ($T_1 = 1563 \pm 40$ ms, precision:121 ms) ($p < 10^{-6}$), which is in accordance with previous literature[13]. No significant difference between MOLLI $T_1$-times acquired in diastole ($T_1 = 1161 \pm 40$ ms, precision:73.5) and in systole ($T_1 = 1160 \pm 55$ ms, precision:62.8 ms) was found (p = 0.8) in this initial cohort. Diastolic SAPPHIRE $T_1$-times ($T_1 = 1577$ ms ± 48 ms, precision:85.5 ms) are significantly higher than systolic SAPPHIRE $T_1$-times ($T_1 = 1563 \pm 40$ ms, precision:121 ms) when the optimized 'systolic parameter set' is used for the latter ($p < 10^{-3}$). Systolic SAPPHIRE $T_1$-times acquired with the 'diastolic parameter set' were higher than the previous

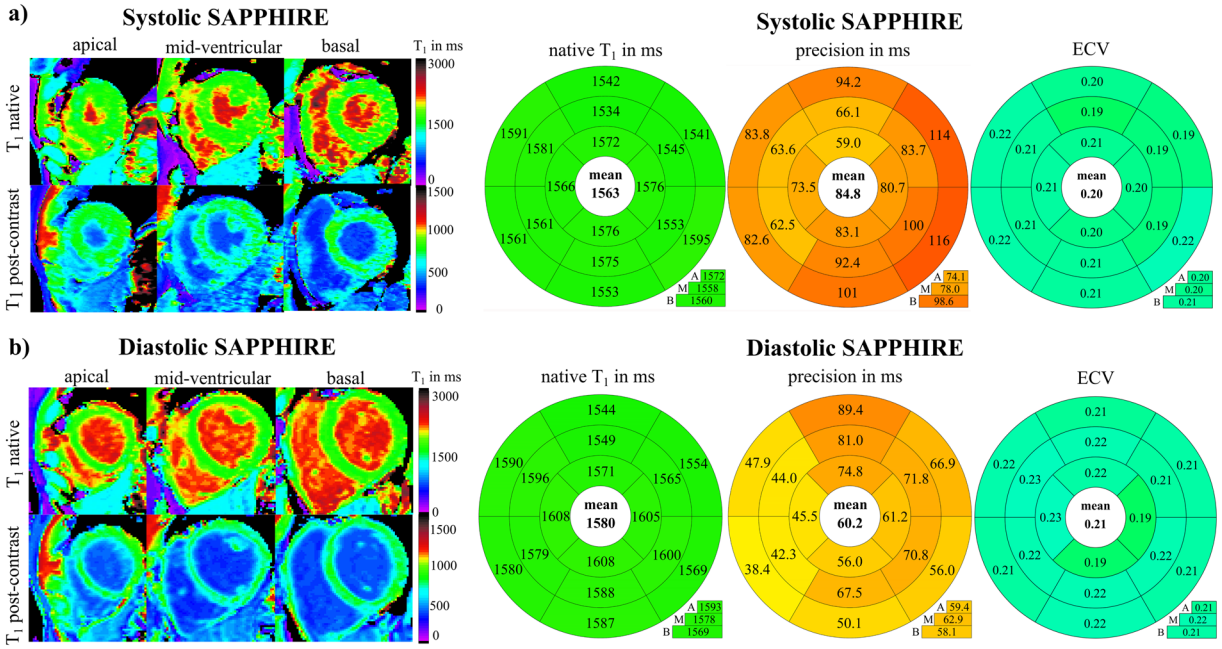


**Figure 5.** The left side shows native and post-contrast $T_1$-maps of a healthy volunteer (m, 35 y), acquired with systolic (**a**) and diastolic (**b**) $T_1$-mapping. $T_1$-map quality is visually high in short axis apical (left), mid-ventricular (middle) and basal (right) slices. Mean values of ten healthy volunteers (5 m, 25 ± 4 y) in three short-axis slices (A = apical, M = mid-ventricular, B = basal) are displayed as bullseye plots (AHA-16-segment-model) for native myocardial $T_1$- times, $T_1$-time precision and ECV, acquired with the systolic SAPPHIRE technique (**a**) and the diastolic SAPPHIRE technique (**b**). The average across all segments is given in the bullseye centers, slice averages in the boxes below.

two ($T_1$ = 1591 ± 84 ms, precision:65.9) in average. However, due to the limited cohort size no significance was found in the differences between systolic and diastolic parameter sets, despite this major difference in the average value. Systolic SAPPHIRE with 15 base images ($T_1$ = 1559 ± 40 ms, precision:120 ms), yielded $T_1$-times comparable to the systolic SAPPHIRE with 10 base images in terms of $T_1$-time and precision ($T_1$ = 1563 ± 40 ms, precision:121 ms) (p = 0.2).

Figure 5 compares *in-vivo* systolic (a) and diastolic (b) pre- and post-contrast SAPPHIRE $T_1$-maps in ten healthy volunteers. Excellent $T_1$-map quality, a high contrast and homogeneous $T_1$-values, indicating high precision, were achieved. Bullseye-plots on the right show that systolic SAPPHIRE $T_1$-times (1563 ± 56 ms, precision: 84.8 ms) are significantly lower than diastolic $T_1$-times (1580 ± 62 ms, precision: 60.2 ms) ($T_1$: p = 0.0124; precision: p = 0.0098). Accordingly, systolic and diastolic ECV-values (0.20 ± 0.03/0.21 ± 0.03) show significant differences (p = 0.03).

Figure 6 depicts all base-images and corresponding $T_1$-maps from a patient suffering from arrhythmia during the scan (c). Due to mis-triggering-induced motion between the base-images, significant artifacts are visible with diastolic SAPPHIRE (b), extending throughout the LV-myocardium and being most severe in the septum. No such artifacts are observed with systolic SAPPHIRE (a), displaying resilience to arrythmia. For both systole and diastole, patient $T_1$ was clearly elevated compared to $T_1$ in healthy, as shown in (d). In patients, mean mid-ventricular systolic $T_1$-values (1582 ± 48 ms) are significantly lower than distolic $T_1$ (1633 ± 74 ms) (p = 0.0311).

## Discussion

In this study, the saturation-recovery $T_1$-mapping sequence SAPPHIRE was modified to robustly measure myocardial $T_1$ during systole in arrhythmic patients. Excellent $T_1$-map quality was achieved in healthy volunteers and arrhythmic patients, despite the short and early systolic acquisition window. In healthy, a significant difference between systolic and diastolic $T_1$- and ECV-values was found, most likely to be explained by reduced partial-volume effects in systole.

Unlike inversion-recovery $T_1$-mapping techniques, SAPPHIRE has predefined delays after saturation and inversion, enabling robust and accurate $T_1$-mapping across subjects with different heart-rates. However, numerical simulations revealed a degrading effect of mis-triggering on diastolic $T_1$-mapping. Accordingly, $T_1$-mapping in arrhythmic patients showed that major variations in diastolic duration led to artifacts. The problem stems from the single fixed trigger-time for multiple image acquisitions: If the diastolic phase shortens significantly during imaging, the trigger-time extends beyond the occurrence of the next R-wave. The systolic phase, however, is not subject to shortening in all common arrhythmias[18], enabling a stationary time for imaging with a lower risk of mis-triggering. However, due to the brevity of the quiescent period and the high myocardial mobility, systolic $T_1$-mapping is performed with shorter acquisition windows to minimize temporal blurring. Diastolic methods

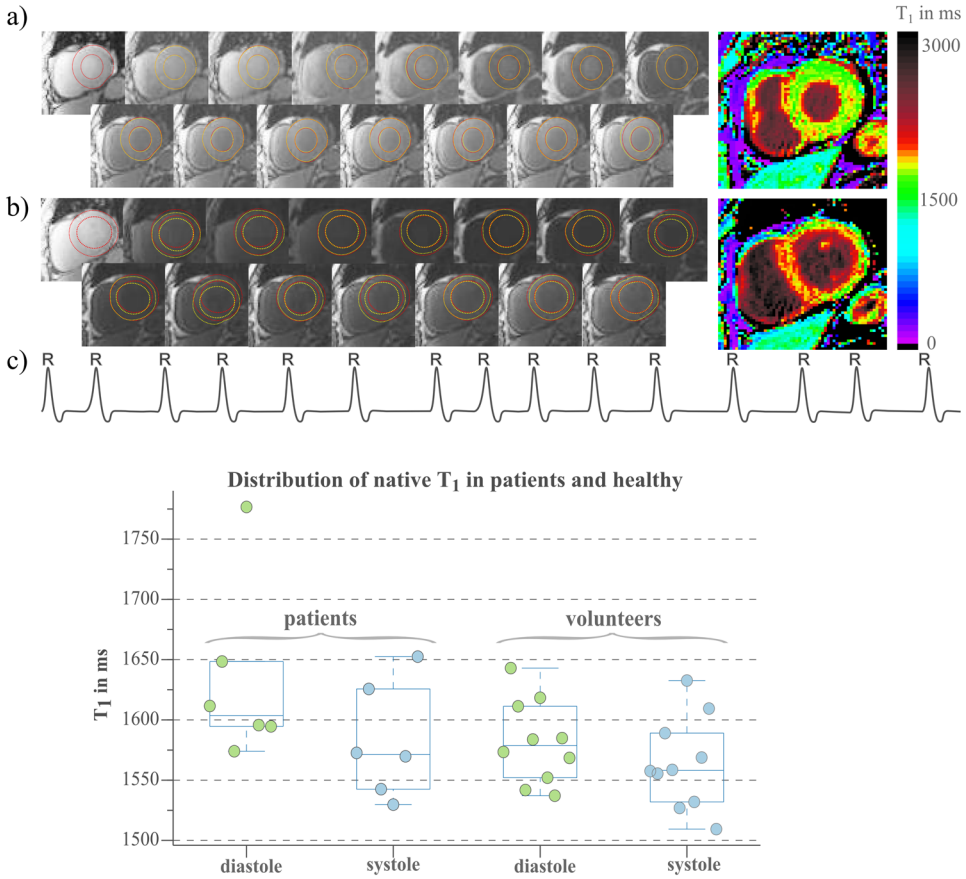


**Figure 6.** SAPPHIRE $T_1$-mapping data in systolic (**a**) and diastolic (**b**) acquisition of a patient (m, 73 y) suffering from arrhythmia. Left ventricular myocardial borders are delineated in red in all 15 recovery images for the myocardial borders of the first cardiac frame, in yellow for all the following frames. In systole, the borders accord with the first frame, which reflects in less artifacts on the $T_1$-map on the right. The detected 15 RR-lengths during that measurement are depicted below (**c**) to visualize the arrhythmia (variability in RR length (RR mean ± std) = 816 ± 134 ms; min: 613 ms; max: 1068 ms). (**d**) Boxplots showing native $T_1$-estimations with systolic and diastolic SAPPHIRE of six patients (4 m, 52 ± 19 y) suffering from arrhythmia and ten healthy volunteers (5 m, 25 ± 4 y). Superimposed scattered data points indicate mean $T_1$ per subject.

commonly employ acquisition windows up to ~360 ms, which extends far beyond systolic quiescence. For systole, a higher GRAPPA-factor (GRAPPA = 3 versus 2) and an increased bandwidth were chosen to reach a temporal resolution of ~160 ms. This trade-off led to decreased precision in systolic $T_1$-maps of healthy volunteers. Future studies will focus on employing advanced acceleration techniques[19,20], potentially exploiting the interdependence between the baseline images[21], in order to mitigate this loss in precision. In systole, moreover, a smaller slice thickness of 6 mm (versus 8 mm in diastole) was chosen to avoid partial volume effects with the high signal from the adjacent blood pool, which is particularly important in systolic imaging as the cardiac long axis is substantially shortened during the contraction. A preliminary comparison in five healthy volunteers between the proposed systolic SAPPHIRE method and the systolic SAPPHIRE method with the 'diastolic parameter set' and only one modified parameter (imaging phase) led to a higher mean value in the latter case. However, due to the small sample size of five volunteers, no statistically significant difference could be shown.

An alternative to mitigate motion artifacts from mis-triggering is image co-registration. However, substantial contrast variations between the base-images hamper the use of conventional methods. Dedicated registration algorithms based on image synthetization[22] or contrast-variation-adapted optical flow[23] have been proposed to improve parameter map quality and decrease spatial variability by alleviating breathing motion effects[24], which are mostly translational. Mis-triggering and imaging during systole, however, are non-translational. Moreover, saturation-recovery yields, compared with inversion-recovery, low baseline SNR, further reducing the effectiveness of registration algorithms[13]. Imaging during systole, on the other hand, robustly ensures image co-registration regardless of baseline SNR and without extensive post-processing with dedicated non-rigid contrast-adapted registration methods.

Usually, to allow fitting of magnitude-images to a parameter model with negative values, base-images are sorted by their TI and point-wise successive flipping of polarity is performed until best fit is reached. In systolic SAPPHIRE, both TI and the saturation-time TS are variable, so this scheme could lead to wrong

polarity assignments for large variations in TS. Therefore, phase-sensitive $T_1$-fitting, as previously proposed for inversion-recovery[25], is performed based on phase-images.

Reported diastolic $T_1$-times are in good agreement with a study on saturation-recovery at 3T[13], which estimated diastolic $T_1$-times of $1578 \pm 42$ ms and ECV-values of $0.20 \pm 0.02$. The present study found systolic SAPPHIRE $T_1$ to be significantly shorter than diastolic SAPPHIRE $T_1$, which agrees with previous studies using systolic MOLLI at 3T[8,26]. As one explanation, Kawel *et al.* presume a lower myocardial blood-volume concentration during systole. A potentially more dominant effect might be the reduction of partial-voluming, achieved by imaging at increased myocardial thickness. This might explain why no significant differences between systolic and diastolic $T_1$ where found in other studies, where only small ROIs were drawn, thoroughly excluding borders and therefore partial-voluming[27]. Yet the comparison of diastolic and systolic MOLLI in the preliminary substudy of this work showed no difference. However, too small of a sample size might have induced lack of significance.

Systolic ECV was found to be significantly lower than diastolic ECV, which is as well in agreement with other publications at 3T[8,26]. Again, this might be due to less partial-voluming with the blood-pool, leading to lower native $T_1$ and higher post-contrast $T_1$, conjointly resulting in a lower ECV for systole.

The present study has several limitations. A relatively small cohort of healthy volunteers, carefully selected to yield healthy myocardium with no age-related diffuse fibrosis, was recruited. Patients were not chosen from this strictly confined age-group and displayed various underlying pathologies, but other types of arrhythmia might also benefit from systolic acquisition. To facilitate integration into the clinical scan protocol, a single native mid-ventricular slice was acquired per patient, preventing segmentation according to the AHA-16-segment-model and ECV-estimation. In future work combination with slice-accelerated imaging will be explored to allow assessment of three left-ventricular slices in the scan protocol[28]. Furthermore, the proposed approach could be readily performed at 1.5T, which remains to be examined in future work.

In conclusion, our results show that the systolic SAPPHIRE saturation-recovery technique facilitates $T_1$-mapping even in patients suffering from arrhythmia. Increased temporal resolution was achieved for the trade-off against slightly reduced precision. Systolic $T_1$-mapping enabled imaging at increased myocardial thickness, resulting in significantly lower systolic $T_1$-times and ECV-values. Hence, the proposed technique might be an alternative to diastolic $T_1$-mapping, for clinical cohorts which displaying substantial variation in the RR-interval.

## References


1. Khan, R. & Sheppard, R. Fibrosis in heart disease: understanding the role of transforming growth factor-β(1) in cardiomyopathy, valvular disease and arrhythmia. *Immunology* **118**, 10–24 (2006).
2. Radenkovic, D., Weingärtner, S., Ricketts, L., Moon, J. C. & Captur, G. $T_1$ mapping in cardiac MRI. *Heart Failure Reviews* **22**, 415–430 (2017).
3. Messroghli, D. R. *et al.* Modified Look-Locker inversion recovery (MOLLI) for high-resolution $T_1$ mapping of the heart. *Magn Reson Med* **52**, 141–146 (2004).
4. Wong, T. C. *et al.* Association Between Extracellular Matrix Expansion Quantified by Cardiovascular Magnetic Resonance and Short-Term Mortality. *Circulation* **126**, 1206–1216 (2012).
5. Kellman, P. & Hansen, M. S. $T_1$-mapping in the heart: accuracy and precision. *J Cardiovasc Magn Reson* **16**, 2 (2014).
6. Weingärtner, S., Meßner, N. M., Zöllner, F. G., Akçakaya, M. & Schad, L. R. Black-blood native $T_1$ mapping: Blood signal suppression for reduced partial voluming in the myocardium. *Magn Reson Med* **78**, 484–493 (2017).
7. Ferreira, V. M. *et al.* Systolic ShMOLLI myocardial $T_1$-mapping for improved robustness to partial-volume effects and applications in tachyarrhythmias. *J Cardiovasc Magn Reson* **17**, 77 (2015).
8. Zhao, L. *et al.* Systolic MOLLI $T_1$ mapping with heart-rate-dependent pulse sequence sampling scheme is feasible in patients with atrial fibrillation. *J Cardiovasc Magn Reson* **18**, 13 (2016).
9. Roujol, S. *et al.* Accuracy, precision, and reproducibility of four $T_1$ mapping sequences: a head-to-head comparison of MOLLI, ShMOLLI, SASHA, and SAPPHIRE. *Radiology* **272**, 683–9 (2014).
10. Weingärtner, S. *et al.* Combined saturation/inversion recovery sequences for improved evaluation of scar and diffuse fibrosis in patients with arrhythmia or heart rate variability. *Magn Reson Med* **71**, 1024–1034 (2014).
11. Chow, K. *et al.* MOLLI $T_1$ Values Have Systematic T2 and Inversion Efficiency Dependent Errors. *Proc Intl Soc Mag Reson Med*, 3288 (2012).
12. Chow, K. *et al.* Saturation recovery single-shot acquisition (SASHA) for myocardial $T_1$ mapping. *Magn Reson Med* **71**, 2082–2095 (2013).
13. Weingärtner, S. *et al.* Myocardial $T_1$-mapping at 3T using saturation-recovery: reference values, precision and comparison with MOLLI. *J Cardiovasc Magn Reson* **18**, 84 (2016).
14. Waktare, J. E. P. Atrial Fibrillation. *Circulation* **106**, 14–16 (2002).
15. Kellman, P., Herzka, D. A. & Hansen, M. S. Adiabatic inversion pulses for myocardial $T_1$ mapping. *Magn Reson Med* **71**, 1428–1434 (2014).
16. Cerqueira, M. D. *et al.* American Heart Association Writing Group on Myocardial Segmentation Registration for Cardiac Imaging: Standardized Myocardial Segmentation and Nomenclature for Tomographic Imaging of the Heart: A Statement for Healthcare Professionals From the Cardiac Imaging Committee of the Council on Clinical Cardiology of the American Heart Association. *Circulation* **105**, 539–542 (2002).
17. Schweser, F., Deistung, A. & Reichenbach, J. R. Foundations of MRI phase imaging and processing for Quantitative Susceptibility Mapping (QSM). *Z Med Phys* **26**, 6–34 (2016).
18. Kobza, R. *et al.* Prevalence of long and short QT in a young population of 41,767 predominantly male Swiss conscripts. *Heart Rhythm* **6**, 652–657 (2009).
19. Marty, B., Coppa, B. & Carlier, P. G. Fast, precise, and accurate myocardial $T_1$ mapping using a radial MOLLI sequence with FLASH readout. *Magn Reson Med* **3**, 26795 (2017).
20. Wang, X. *et al.* Model-based $T_1$ mapping with sparsity constraints using single-shot inversion-recovery radial FLASH. *Magn Reson Med* **11**, 26726 (2017).
21. Moeller, S., Weingärtner, S. & Akçakaya, M. Multi-scale locally low-rank noise reduction for high-resolution dynamic quantitative cardiac MRI. In *Conf Proc IEEE Eng Med Biol Soc,* 1473–1476 (2017).
22. Xue, H. *et al.* Motion correction for myocardial $T_1$ mapping using image registration with synthetic image estimation. *Magn Reson Med* **67**, 1644–1655 (2012).
23. Roujol, S. *et al.* Adaptive registration of varying contrast-weighted images for improved tissue characterization (ARCTIC): application to $T_1$ mapping. *Magn Reson Med* **73**, 1469–82 (2015).

24. Roujol, S. *et al.* Impact of motion correction on reproducibility and spatial variability of quantitative myocardial T2 mapping. *J Cardiovasc Magn Reson* **17**, 46 (2015).
25. Xue, H. *et al.* Phase-sensitive inversion recovery for myocardial $T_1$ mapping with motion correction and parametric fitting. *Magn Reson Med* **69**, 1408–1420 (2013).
26. Kawel, N. *et al.* $T_1$ mapping of the myocardium: intra-individual assessment of the effect of field strength, cardiac cycle and variation by myocardial region. *J Cardiovasc Magn Reson* **14**, 27 (2012).
27. Weingärtner, S. *et al.* Temporally resolved parametric assessment of Z-magnetization recovery (TOPAZ): Dynamic myocardial $T_1$ mapping using a cine steady-state look-locker approach. *Magn Reson Med* **79**, 2087–2100 (2018).
28. Weingärtner, S. *et al.* Simultaneous multislice imaging for native myocardial $T_1$ mapping: Improved spatial coverage in a single breath-hold. *Magn Reson Med* **78**, 462–471 (2017).

## Acknowledgements

We would like to thank Uwe Mattler for his support with image acquisition. We acknowledge the financial support of the Deutsche Forschungsgemeinschaft and Ruprecht-Karls-Universität Heidelberg within the funding programme Open Access Publishing.

## Author Contributions

All authors read and approved the final manuscript. NMM was responsible for study conception, design and organization, data acquisition in phantoms and volunteers, analysis, statistical analysis and interpretation of data, writing of the main manuscript text, preparation of all figures, and manuscript revision and finalizing. JB participated in study conception, patient and clinical concerns during study realization, data interpretation, and manuscript revision. DL participated in study conception and revised the manuscript for medical content. TP participated in study conception and was as clinical investigator responsible for medical and clinical concerns during study realization, data interpretation, and manuscript revision. LRS contributed by overseeing the study and editing various drafts of the manuscript. FGZ was responsible for study ethics and organizational matters, conception and design of the study, and critically revised the manuscript. SW performed sequence implementation and was engaged in conception and design of the study, data acquisition in phantoms and volunteers, as well as the interpretation of data and manuscript revising.

## Additional Information

**Competing Interests:** Dr. Sebastian Weingärtner has the following conflict of interest to declare: S.W. is inventor of a pending U.S. and European patent entitled "Methods for scar imaging in patients with arrhythmia". There are no further conflicts of interest to declare.

**Publisher's note:** Springer Nature remains neutral with regard to jurisdictional claims in published maps and institutional affiliations.